





(GE Healthcare) was prepared with 50 mM HEPES pH 7.4 and 150 mM NaCl at a concentration of 50  $\mu$ M was used.

## 2.6. Denaturing PAGE

To prove the presence of RNA in preformed gels, soaking experiments, the crystals were dissolved in denaturing buffer. The samples were analyzed via denaturing polyacrylamide gel electrophoresis. The samples were carried out on 18% polyacrylamide gels buffered with TBE for 1 h at 20 W. Images were captured using a ChemiDoc MP System (BioRad, Hercules, CA).

### 2.7. Small angle X-ray scattering

The scattering patterns were recorded on a SAXS system “Ganesha-Air” from Forschungszentrum Jülich. The X-ray source was a microfocus tube (Xc3000, Excillum) with a liquid metal anode (Ga) with Ga-K $\alpha$  radiation (wavelength  $\lambda = 0.141$  nm). The beam was brilliant and a very small beam ( $< 20$   $\mu$ m). The sample was from Baden-Daettwil, Switzerland) was used. The scattering patterns. All samples were sealed in a 0.5 mm diameter. Data were circular averaged and background and transmission corrected. The scattering was measured at a detector distance of 1.5 m. The data were from factor concentrations of 5, 10, 20, 30, 40, 50, 60, 70, 80, 90, 100, 110, 120, 130, 140, 150, 160, 170, 180, 190, 200, 210, 220, 230, 240, 250, 260, 270, 280, 290, 300, 310, 320, 330, 340, 350, 360, 370, 380, 390, 400, 410, 420, 430, 440, 450, 460, 470, 480, 490, 500, 510, 520, 530, 540, 550, 560, 570, 580, 590, 600, 610, 620, 630, 640, 650, 660, 670, 680, 690, 700, 710, 720, 730, 740, 750, 760, 770, 780, 790, 800, 810, 820, 830, 840, 850, 860, 870, 880, 890, 900, 910, 920, 930, 940, 950, 960, 970, 980, 990, 1000, 1010, 1020, 1030, 1040, 1050, 1060, 1070, 1080, 1090, 1100, 1110, 1120, 1130, 1140, 1150, 1160, 1170, 1180, 1190, 1200, 1210, 1220, 1230, 1240, 1250, 1260, 1270, 1280, 1290, 1300, 1310, 1320, 1330, 1340, 1350, 1360, 1370, 1380, 1390, 1400, 1410, 1420, 1430, 1440, 1450, 1460, 1470, 1480, 1490, 1500, 1510, 1520, 1530, 1540, 1550, 1560, 1570, 1580, 1590, 1600, 1610, 1620, 1630, 1640, 1650, 1660, 1670, 1680, 1690, 1700, 1710, 1720, 1730, 1740, 1750, 1760, 1770, 1780, 1790, 1800, 1810, 1820, 1830, 1840, 1850, 1860, 1870, 1880, 1890, 1900, 1910, 1920, 1930, 1940, 1950, 1960, 1970, 1980, 1990, 2000, 2010, 2020, 2030, 2040, 2050, 2060, 2070, 2080, 2090, 2100, 2110, 2120, 2130, 2140, 2150, 2160, 2170, 2180, 2190, 2200, 2210, 2220, 2230, 2240, 2250, 2260, 2270, 2280, 2290, 2300, 2310, 2320, 2330, 2340, 2350, 2360, 2370, 2380, 2390, 2400, 2410, 2420, 2430, 2440, 2450, 2460, 2470, 2480, 2490, 2500, 2510, 2520, 2530, 2540, 2550, 2560, 2570, 2580, 2590, 2600, 2610, 2620, 2630, 2640, 2650, 2660, 2670, 2680, 2690, 2700, 2710, 2720, 2730, 2740, 2750, 2760, 2770, 2780, 2790, 2800, 2810, 2820, 2830, 2840, 2850, 2860, 2870, 2880, 2890, 2900, 2910, 2920, 2930, 2940, 2950, 2960, 2970, 2980, 2990, 3000, 3010, 3020, 3030, 3040, 3050, 3060, 3070, 3080, 3090, 3100, 3110, 3120, 3130, 3140, 3150, 3160, 3170, 3180, 3190, 3200, 3210, 3220, 3230, 3240, 3250, 3260, 3270, 3280, 3290, 3300, 3310, 3320, 3330, 3340, 3350, 3360, 3370, 3380, 3390, 3400, 3410, 3420, 3430, 3440, 3450, 3460, 3470, 3480, 3490, 3500, 3510, 3520, 3530, 3540, 3550, 3560, 3570, 3580, 3590, 3600, 3610, 3620, 3630, 3640, 3650, 3660, 3670, 3680, 3690, 3700, 3710, 3720, 3730, 3740, 3750, 3760, 3770, 3780, 3790, 3800, 3810, 3820, 3830, 3840, 3850, 3860, 3870, 3880, 3890, 3900, 3910, 3920, 3930, 3940, 3950, 3960, 3970, 3980, 3990, 4000, 4010, 4020, 4030, 4040, 4050, 4060, 4070, 4080, 4090, 4100, 4110, 4120, 4130, 4140, 4150, 4160, 4170, 4180, 4190, 4200, 4210, 4220, 4230, 4240, 4250, 4260, 4270, 4280, 4290, 4300, 4310, 4320, 4330, 4340, 4350, 4360, 4370, 4380, 4390, 4400, 4410, 4420, 4430, 4440, 4450, 4460, 4470, 4480, 4490, 4500, 4510, 4520, 4530, 4540, 4550, 4560, 4570, 4580, 4590, 4600, 4610, 4620, 4630, 4640, 4650, 4660, 4670, 4680, 4690, 4700, 4710, 4720, 4730, 4740, 4750, 4760, 4770, 4780, 4790, 4800, 4810, 4820, 4830, 4840, 4850, 4860, 4870, 4880, 4890, 4900, 4910, 4920, 4930, 4940, 4950, 4960, 4970, 4980, 4990, 5000, 5010, 5020, 5030, 5040, 5050, 5060, 5070, 5080, 5090, 5100, 5110, 5120, 5130, 5140, 5150, 5160, 5170, 5180, 5190, 5200, 5210, 5220, 5230, 5240, 5250, 5260, 5270, 5280, 5290, 5300, 5310, 5320, 5330, 5340, 5350, 5360, 5370, 5380, 5390, 5400, 5410, 5420, 5430, 5440, 5450, 5460, 5470, 5480, 5490, 5500, 5510, 5520, 5530, 5540, 5550, 5560, 5570, 5580, 5590, 5600, 5610, 5620, 5630, 5640, 5650, 5660, 5670, 5680, 5690, 5700, 5710, 5720, 5730, 5740, 5750, 5760, 5770, 5780, 5790, 5800, 5810, 5820, 5830, 5840, 5850, 5860, 5870, 5880, 5890, 5900, 5910, 5920, 5930, 5940, 5950, 5960, 5970, 5980, 5990, 6000, 6010, 6020, 6030, 6040, 6050, 6060, 6070, 6080, 6090, 6100, 6110, 6120, 6130, 6140, 6150, 6160, 6170, 6180, 6190, 6200, 6210, 6220, 6230, 6240, 6250, 6260, 6270, 6280, 6290, 6300, 6310, 6320, 6330, 6340, 6350, 6360, 6370, 6380, 6390, 6400, 6410, 6420, 6430, 6440, 6450, 6460, 6470, 6480, 6490, 6500, 6510, 6520, 6530, 6540, 6550, 6560, 6570, 6580, 6590, 6600, 6610, 6620, 6630, 6640, 6650, 6660, 6670, 6680, 6690, 6700, 671

## 2.8. NMR spectra

NMR ac  
HD + spectr  
and equippe  
cryoprobe  
2048x512  
200  $\mu$ M  
in 50 m  
v) D<sub>2</sub>O  
plott

## 2.9

coordinates for the U1A  
collaboratory for Struc-  
B PDB) ([Berman, 2000](#)).  
for the reported crystal

R70W, 6SR7 for the obtained by soaking, and 6SON for

### 3. Results

### 3.1. Design, biosynthesis, and characterization of

To identify amino acid positions that likely affect the RNA-binding properties of U1A we used a BLAST search (Altschul *et al.*, 1990) to search for U1A-RBD homologs from other species. Whereas most U1A-RBDs from Archaea and Bacteria have conserved amino acid residues, most homologs from *Viridiplantae* contain a conserved phenylalanine at position 56 (Fig. S1). This Phe is important for the RNA-RBD RNA binding as the phenylalanine stacks with the 5'-terminal adenosine of the RNA complex formed by U1A and RNA (Shiels *et al.*, 2005). The Phe56 RNA hairpin sequence is conserved in U1A-RBDs from other species, which indicates that the mutation F56W shown in Fig. 1B is likely to affect the RNA binding of U1A-RBD (Law, 2005; Shiels *et al.*, 2005). To study the effect of this mutation, we exchanged the amino acid residue at position 56 for a tryptophan, which indicates that the exchange of amino acid residues at positions 56 and 31 affects the crystallization behavior and the protein stability (Price *et al.*, 1995). Since an U1A variant with a double mutation F56W and Y31H and Q36R has been reported (Price *et al.*, 1995), we exchanged the properties compared to the wildtype. To study the effect of this mutation, we used this double mutant as a positive control for all tryptophan mutations. In addition, we exchanged the amino acid residues A2, H10, R70, and K98 in the RNA binding site, since they are located close to the RNA on the protein surface (Fig. 1B). To study the effect of these mutations within the expression plasmid, we exchanged the amino acid sequence, we exchanged the amino acid residues A2, R70, and K98 by W using a site-directed mutagenesis. The proteins were then expressed in *E. coli* and purified in high yields. All proteins were purified to high purity using a combination of ion exchange chromatography steps (Fig. S2).

Next, we tested the ability of the *in vitro* selected RNA hairpins to bind RNA. The RNA hairpin sequences were synthesized and analyzed the sample by size exclusion chromatography and electrophoretic mobility shift assay (EMSA) to determine if they bind RNA in solution.

[illegible]



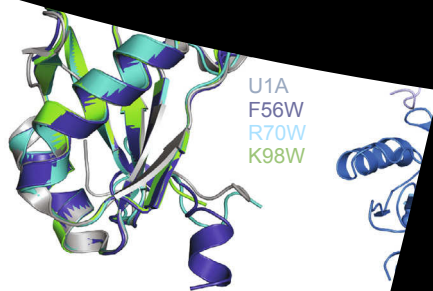


**Fig. 3.** Crystal structures of U1A triple mutants in blue; R70W in cyan, and K98W in green. Biological assembly of the triple mutant R70W K98W (D). Residues 56 and 92 are shown as sticks.

excess electron density close to the C-terminus may indicate a partial formation of helix C. The conformational rearrangement in U1A variant K98W may be induced by the C-terminal residues on protein-protein interactions.

### 3.4. Binding of U1A variants to the U1 snRNA

To ameliorate the process of growth, we established a protocol for soaking the hairpin motif in combination with the success of RNA binding exploiting the tryptophan residue. We produced R70W and K98W, which did not radiate with UV light (Fig. 4). These crystals with a solution of the motif. The RNA sequence contained a characteristic hairpin motif of the U1A protein (Table 1). The light shows that the crystals do not quench (Fig. 4, middle). Crystals with the U1A protein show fluorescence in case of the tryptophan residue. We speculate that the loss of fluorescence quenching depends on the tryptophan residue at position 70, as a consequence of a change in the conformation of the hairpin motif.

To validate the RNA binding to the RNA sequence of binding to crystals retained RNA. In comparison formed R72 mutation in fl

To  
binding  
specific  
loading  
nuc  
so  
p

proteins of the U1A family are all capable of binding to the same target, only the F56W mutant is able to bind to the target *in crystallo*.







Writing - original dra.

The authors declare that they have no known competing financial interests or personal relationships that could have influenced the work reported in this paper.

This work was supported by the Funds of 196/05 to I.S. and Hoe 700080 to H.R.]; the schen Volkes [to H.R.]; and the Deutsche 103/2, ET 103/4 to M.E.]. We acknowledge (Germany), a member of the Helmholtz vision of experimental facilities. Parts of at PETRA III and we would like to thank and Eva Crosas for assistance in using beamline P11. We gratefully acknowledge with the data processing and modeling assisting with the analytical SEC experiments. Wördehoff for assisting with the project. Stefanie Kobus from the Center for DFG, grant number 417919780) for

Supplementary data to this article are available at [doi.org/10.1016/j.jsb.2020.100000](https://doi.org/10.1016/j.jsb.2020.100000).

Adams, P.L., Stahley, M.R., Kosev  
a self-splicing group I intron  
Altschul, S.F., Gish, W., Miller, W.,  
search tool. J. Mol. Biol. 257, 105-132.  
Berman, H.M., 2000. The protein  
Bernhart, S.H., Tafer, H., Mikolajczyk  
Partition function and base pairing  
Mol. Biol. 1, 3.  
Burke, J.E., Butcher, S.E., 1997. X-ray  
ray scattering (SAXS) studies of  
Burkhardt, A., Pakendorf, J., Schmitt  
S., Lorbeer, O., Strohriegl, P., 2002.  
Status of the crystallographic  
Cochrane, J.C., Lipchik, D.L., 1997.  
ribozyme bound to a small-molecule  
Emsley, P., Cowtan, K., 2001. Data  
Crystallogr. Sci. Technol. 1, 12-20.  
Ferré-D'Amaré, A., 2000. The  
structure determined by X-ray  
Access, pp. 1-12. <http://www.rcsb.org/pdb>.  
Ferré-D'Amaré, A., 2001. The  
lization of small-molecule  
Ferré-D'Amaré, A., 2002. The  
Nucleic Acids Res. 30, 1-12.  
Ferré-D'Amaré, A., 2003. The  
hepatitis delta virus (HDV) RNA  
lization of small-molecule  
Ferré-D'Amaré, A., 2004. The  
viral RNA sequences.  
Franz, A., 2005. The  
sequences.

Acta Crystallogr.

Journal of Archaeological Science 122 (2019) 105154

sequence requirements in the 1990s. *Journal of Interpersonal Violence*, 27, 40617–40622.